Paper 102

©Civil-Comp Press, 2012
Proceedings of the Eleventh International Conference
on Computational Structures Technology,
B.H.V. Topping, (Editor),
Civil-Comp Press, Stirlingshire, Scotland

Free Vibration of a Functionally Graded Timoshenko Beam using the Dynamic Stiffness Method

H. Su[1] and J.R. Banerjee[2]
[1] School of Science and Technology
University of Northampton, United Kingdom
[2] School of Engineering and Mathematical Sciences
City University London, United Kingdom

Abstract

The dynamic stiffness method is used to investigate the free vibration behaviour of a functionally graded beam (FGB). The material properties of the FGB are assumed to vary in the thickness direction based on a power-law. The kinetic and potential energies of the beam are formulated using the Timoshenko beam theory. The governing differential equations of motion in free vibration for the FGB are derived using Hamilton's principle. The analytical expressions for axial force, shear force and bending moments at any cross-section of the FGB are obtained as a by-product of the Hamiltonian formulation. The differential equations are solved in closed analytical form for harmonic oscillation. The dynamic stiffness matrix of the FGB is then formulated by relating the amplitudes of forces and displacements at the ends of the beam. The Wittrick-Williams algorithm is used as solution technique to yield natural frequencies and mode shapes of the FGB. A parametric study is carried out by varying significant beam parameters and boundary conditions. The investigation required a substantial amount of validation exercise to confirm the predictable accuracy of the dynamic stiffness method. The results are discussed and some concluding remarks are made.

Keywords: free vibration, functionally graded beams, dynamic stiffness method, Wittrick-Williams algorithm, Timoshenko beam theory.

1 Introduction

Functionally graded materials (FGM), which have continuous transition of material properties as a function of position along certain directions, are regarded most promising for future application of advanced composites against the backdrop of traditional isotropic and homogeneous materials. The gradual variation of material properties can be tailored to suit different purposes in engineering which is a great advantage of using FGM. Design of aircraft and space vehicles structures, electronic and biomedical installations are some examples where FGM can be exploited to advantage. It is thus important to understand the static and dynamic behaviour of structural components made from FGM. In this way, the analysis of FGM structures has attracted many researchers in recent years. Of particular interest, are beam structures which are widely used in aeronautical, civil, mechanical and other installations as principal load carrying members. The dynamic behaviour of the functionally graded beams (FGB) in particular has become an area of intense research activity and the literature is steadfastly growing [1-11]. Some researchers have used traditional finite element and other approximate methods. Side by side to such developments, Bernoulli-Euler, Timoshenko, and/or higher order shear deformation beam theories leading to the development of frequency equations have also been reported. Apparently, there has not been any attempt to solve the problem using the dynamic stiffness method (DSM). The purpose of this research is to fill this gap in the literature by applying the DSM to investigate the free vibration behaviour of FGB. The proposed DSM uses exact member theory based on frequency dependent shape functions obtained from the exact solution of the governing differential equations of motion of the FGB in its free vibration. The method provides exact results for all natural frequencies and mode shapes of the FGB without making any approximation en route. The DSM is recognizably more accurate than the traditional finite element and other approximate methods.

The investigation is carried out in following steps. First the material properties of the FGB are chosen to vary through the thickness of the beam according to a power law. The kinetic and potential energies of the FGB are then formulated by using the Timoshenko beam theory which accounts for the effects of shear deformation and rotary inertia. Next, the governing differential equations of motion in free vibration are derived using Hamilton's principle and making use of symbolic computation [12]. The expressions for axial force, shear force and bending moment at any cross-section of the FGB are obtained as a by-product of the Hamiltonian formulation. For harmonic oscillation, the governing differential equations are solved in closed analytical form for axial displacement, bending displacement and bending rotation. Expressions for axial force, shear force and bending moment are also obtained in explicit analytical form by using the solutions of the governing differential equations. The boundary conditions for displacements and forces are imposed in algebraic form to derive the dynamic stiffness matrix of the FGB relating the amplitudes of the forces to those of the displacements. Once the frequency dependent dynamic stiffness matrix of the FGB is developed, the eigenvalue problem is solved by applying the well-established algorithm of Wittrick and Williams [13] to yield natural frequencies and mode shapes of the FGB. The investigation required a substantial amount of validation exercise for which computed results from the present theory are compared with the ones available in the literature. A parametric study is carried out by varying significant beam parameters, such as the length to thickness ratio and the effect of power law distribution. Numerical results are discussed and this is followed by some concluding remarks.

2 Theory

2.1 Derivation of the governing differential equations

Figure 1 shows a uniform FGB with a rectangular cross section in a right-handed Cartesian coordinate system. The beam has a length L, width b, and thickness h. The mechanical properties of the beam are Young's modulus E, Poisson's ratio ν, shear modulus G, and mass density ρ. It is assumed that the material properties of the beam vary continuously in the thickness direction (Z) according to a power law distribution as follows [1]:

$$P(z) = (P_t - P_b)\left(\frac{z}{h} + \frac{1}{2}\right)^k + P_b \tag{1}$$

where P_t and P_b are respectively the material properties at the top and bottom surfaces of the FGB, k is a non-negative parameter which dictates the material variation profile through the thickness of the beam. Three special cases can be observed from the above equation. Clearly $k = 1$ indicates the linear variation of the composition of the top and bottom surfaces of the FGB, $k = 0$ represents the FGB made of full material of the top surface whereas $k = \infty$ represents the FGB made of full material of the bottom surface.

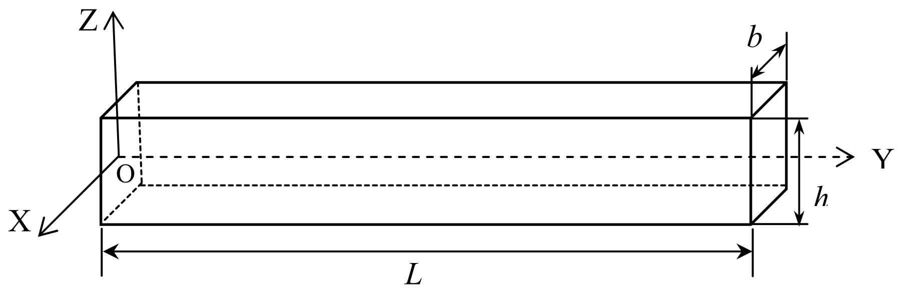

Figure 1: The co-ordinate system and notation for a FGB

Displacements v_1 and w_1 along the Y and Z directions of a point on the cross-section are given by

$$v_1(y,z,t) = v(y,t) - z\frac{\partial w(y,t)}{\partial y} + \varphi(z)\psi(y,t) \tag{2}$$

$$w_1(y,z,t) = w(y,t) \tag{3}$$

where v and w are the corresponding displacements of the point on the neutral axis which may or may not be the middle surface. $\varphi(z)$ in Equation (2) is a function which characterises the distribution of the transverse shear stress through the thickness of the beam and can be ascertained using different beam theories. In the current investigation, the first-order shear deformation beam theory is used which assumes constant shear stress and shear strain in the cross-section and therefore, $\varphi(z) = z$ in Equation (2). Thus the transverse shear strain $\psi(z)$ at any point on the neutral axis can be expressed as

$$\psi(y,t) = \frac{\partial w(y,t)}{\partial y} - \phi(y,t) \tag{4}$$

where ϕ is the total bending rotation of the cross-sections at any point on the neutral axis which is taken to be an unknown function. Equation (2) with the help of Equation (4) becomes

$$v_1(y,z,t) = v(y,t) - z\phi(y,t) \tag{5}$$

The normal and shear strains in the usual notation are:

$$\varepsilon_{yy} = \frac{\partial v_1}{\partial y} = \frac{\partial v}{\partial y} - z\frac{\partial \phi}{\partial y}, \qquad \gamma_{yz} = \frac{\partial v_1}{\partial z} + \frac{\partial w_1}{\partial y} = \frac{\partial w}{\partial y} - \phi \tag{6}$$

Assuming that the material of FGB obeys Hooke's law, the stresses in the beam can be expressed as:

$$\sigma_{yy} = E(z)\varepsilon_{yy}, \; \tau_{yz} = G(z)\gamma_{yz} \tag{7}$$

The potential and kinetic energies of the FGB using Timoshenko beam theory are in the usual notation given by

$$\begin{aligned} U &= \frac{1}{2}\int (\sigma_{yy}\varepsilon_{yy} + \tau_{yz}\gamma_{yz})dV \\ &= \frac{1}{2}\int_0^L \left\{A_0 v'^2 - 2A_1 v'\phi' + A_2\phi'^2\right\}dy + \frac{1}{2}\int_0^L A_3\left\{w'^2 - 2w'\phi + \phi^2\right\}dy \end{aligned} \tag{8}$$

$$T = \frac{1}{2}\int_0^L \left\{\int \rho(z)(\dot{v}_1^2 + \dot{w}_1^2)\right\}dA\,dy = \frac{1}{2}\int_0^L \left\{I_0(\dot{v}^2 + \dot{w}^2) - 2I_1\dot{v}\dot{\phi} + I_2\dot{\phi}^2\right\}dy \tag{9}$$

where a prime and an over dot represent differentiation with respect to space *y* and time *t* respectively.

Property parameters $A_i \; (i = 0, 1, 2, 3)$ and $I_i \; (i = 0, 1, 2)$ appearing in Equations (8) and (9) are defined as:

$$\left.\begin{aligned}\{I_0, I_1, I_2\} &= \int \{1, z, z^2\}\rho(z)dA \\ \{A_0, A_1, A_2\} &= \int \{1, z, z^2\}E(z)dA \\ A_3 &= \int G(z)dA\end{aligned}\right\} \tag{10}$$

Hamilton's principle states

$$\delta\int_{t_1}^{t_2} (T-U)\,dt = 0 \tag{11}$$

where t_1 and t_2 are the time intervals in the dynamic trajectory, and δ is the usual variational operator.

Substituting T and U from Equations (8) and (9) into Equation (11), using the δ operator, integrating each term by parts, and then collecting terms yield the governing differential equations and natural boundary conditions in free vibration of the FGB. The entire procedure has been processed through the application of symbolic computation [12]. The following governing differential equations are eventually obtained as,

$$\left.\begin{aligned}&-I_0\ddot{v} + A_0 v'' + I_1\ddot{\phi} - A_1\phi'' = 0 \\ &-I_0\ddot{w} + A_3 w'' - A_3\phi' = 0 \\ &I_1\ddot{v} - A_1 v'' + A_3 w' - I_2\ddot{\phi} + A_2\phi'' - A_3\phi = 0\end{aligned}\right\} \tag{12}$$

As a by-product of the Hamiltonian formulation, the natural boundary conditions are also obtained analytically to give the expressions for axial force, shear force and bending moment as,

$$F = -A_0 v' + A_1\phi' \tag{13}$$

$$S = -A_3 w' + A_3\phi \tag{14}$$

$$M = A_1 v' - A_2\phi' \tag{15}$$

Assuming harmonic oscillation so that

$$v(y,t) = V(y)e^{i\omega t}\,,\; w(y,t) = W(y)e^{i\omega t}\,,\; \phi(y,t) = \Phi(y)e^{i\omega t} \tag{16}$$

where $V(y)$, $W(y)$ and $\Phi(y)$ are amplitudes of v, w and ϕ, and ω is angular or circular frequency. Introducing the differential operator $D = d/d\xi$ and the non-dimensional length ξ as:

$$\xi = x/L \tag{17}$$

The differential equations of motion of Equation (12) can now be transformed into following forms:

$$\left.\begin{aligned}
&I_0\omega^2L^2V + A_0D^2V - I_1\omega^2L^2\Phi - A_1D^2\Phi = 0\\
&I_0\omega^2L^2W + A_3D^2W - A_3LD\Phi = 0\\
&-I_1\omega^2L^2V - A_1D^2V + A_3LDW + (I_2\omega^2 - A_3)L^2\Phi + A_2D^2\Phi = 0
\end{aligned}\right\} \tag{18}$$

The above three equations can be combined into one sixth order ordinary differential equation, which satisfies each of $V(\xi)$, $W(\xi)$ and $\Phi(\xi)$ as follows,

$$(D^6 + aD^4 + bD^2 + c)H = 0 \tag{19}$$

where

$$H = V(\xi) \text{ or } W(\xi) \text{ or } \Phi(\xi) \tag{20}$$

and

$$\left.\begin{aligned}
&a = \frac{A_0A_2I_0 - A_1^2I_0 + A_0A_3I_2 - 2A_1A_3I_1 + A_2A_3I_0}{(A_0A_2 - A_1^2)A_3}L^2\omega^2\\
&b = \frac{A_2I_0^2\omega^2 - A_3I_1^2\omega^2 - A_0A_3I_0 - 2A_1I_0I_1\omega^2 + A_0I_0I_2\omega^2 + A_3I_0I_2\omega^2}{(A_0A_2 - A_1^2)A_3}L^4\omega^2\\
&c = \frac{-I_1^2\omega^2 + I_0I_2\omega^2 - A_3I_0}{(A_0A_2 - A_1^2)A_3}L^6\omega^4I_0
\end{aligned}\right\} \tag{21}$$

Equation (19) can be reduced to a cubic equation and solved analytically to obtain the three roots of the cubic and hence the six roots r_j $(j = 1,2,\ldots,6)$ of the auxiliary equation. Therefore, the solution of the differential equation (19) can be obtained as:

$$U(\xi) = \sum_{j=1}^{6} P_j e^{r_j\xi},\ V(\xi) = \sum_{j=1}^{6} Q_j e^{r_j\xi},\ \Phi(\xi) = \sum_{j=1}^{6} R_j e^{r_j\xi} \tag{22}$$

where P_j, Q_j and R_j $(j = 1,2,\ldots,6)$ are three different sets of six constants. The constants P_j, Q_j and R_j are not all independent and can be related to each other. The choice of relating two sets of the six constants in terms of the third one is arbitrary. Here, R_j is chosen to be the basic set of constants to which P_j and Q_j are related. When Equations (22) are substituted into Equations (18) we obtain,

$$P_j = \frac{I_1\omega^2 L^2 + A_1 r_j^2}{I_0\omega^2 L^2 + A_0 r_j^2} R_j = \alpha_j R_j, \qquad Q_j = \frac{A_3 L r_j}{I_0\omega^2 L^2 + A_3 r_j^2} R_j = \beta_j R_j \tag{23}$$

Similarly the expressions for the amplitudes of the axial, shear forces and bending moment are also obtained in terms of the constant R_j as,

$$F = \frac{1}{L}(A_1\Phi' - A_0 V') = \frac{1}{L}(A_1\sum_{j=1}^{6} r_j - A_0\sum_{j=1}^{6}\alpha_j r_j)R_j e^{r_j\xi} \tag{24}$$

$$S = \frac{A_3}{L}(-W' + L\Phi) = \frac{A_3}{L}(L - \sum_{j=1}^{6}\beta_j r_j)R_j e^{r_j\xi} \tag{25}$$

$$M = \frac{1}{L}(A_1 V' - A_2\Phi') = \frac{1}{L}(A_1\sum_{j=1}^{6}\alpha_j r_j - A_2\sum_{j=1}^{6} r_j)R_j e^{r_j\xi} \tag{26}$$

2.2 Dynamic stiffness formulation

The dynamic stiffness matrix of the FGB can now be derived by applying boundary conditions for displacements and forces at the ends of the beam. Figure 2 shows the sign convention for axial force, shear force and bending moment used in this paper when applying for the boundary conditions.

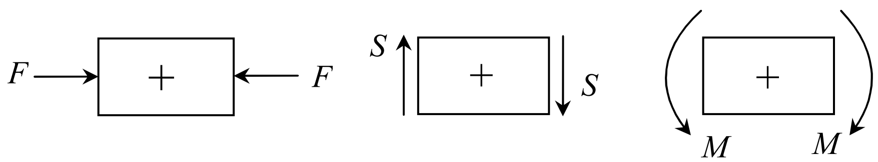

Figure 2: Sign convention for positive axial force, shear force and bending moment.

The boundary conditions for the displacements at the ends of the FGB are,

$$\left.\begin{array}{l} y = 0\ (\xi = 0):\ V = V_1, W = W_1, \Phi = \Phi_1 \\ y = L\ (\xi = 1):\ V = V_2, W = W_2, \Phi = \Phi_2 \end{array}\right\} \tag{27}$$

The boundary conditions for the forces at the both ends of the FGB are,

$$\left.\begin{array}{l} y = 0\ (\xi = 0):\ F = F_1, S = S_1, M = M_1 \\ y = L\ (\xi = 1):\ F = -F_2, S = -S_2, M = -M_2 \end{array}\right\} \tag{28}$$

The matrix relationship between the displacement vector and the six constants R_j can be obtained by substituting Equations (27) into Equations (22) to give

$$
\begin{bmatrix} V_1 \\ W_1 \\ \Phi_1 \\ V_2 \\ W_2 \\ \Phi_2 \end{bmatrix} = \begin{bmatrix} \alpha_1 & \alpha_2 & \alpha_3 & \alpha_4 & \alpha_5 & \alpha_6 \\ \beta_1 & \beta_2 & \beta_3 & \beta_4 & \beta_5 & \beta_6 \\ 1 & 1 & 1 & 1 & 1 & 1 \\ \alpha_1 e^{r_1} & \alpha_2 e^{r_2} & \alpha_3 e^{r_3} & \alpha_4 e^{r_4} & \alpha_5 e^{r_5} & \alpha_6 e^{r_6} \\ \beta_1 e^{r_1} & \beta_2 e^{r_2} & \beta_3 e^{r_3} & \beta_4 e^{r_4} & \beta_5 e^{r_5} & \beta_6 e^{r_6} \\ e^{r_1} & e^{r_2} & e^{r_3} & e^{r_4} & e^{r_5} & e^{r_6} \end{bmatrix} \begin{bmatrix} R_1 \\ R_2 \\ R_3 \\ R_4 \\ R_5 \\ R_6 \end{bmatrix} \tag{29}
$$

or,

$$
\boldsymbol{\delta} = \mathbf{B}\,\mathbf{R} \tag{30}
$$

Similarly the relationship between the force vector and the six constants R_j can be obtained by substituting Equations (28) into Equations (24) – (26) to give

$$
\mathbf{P} = \mathbf{A}\,\mathbf{R} \tag{31}
$$

where

$$
\mathbf{P} = [\, F_1 \;\; S_1 \;\; M_1 \;\; F_2 \;\; S_2 \;\; M_2 \,]^{\mathrm{T}} \tag{32}
$$

with T denoting a transpose. The elements of the **A** matrix in Equation (31) are given by,

$$
\left.
\begin{aligned}
& a_{1j} = \frac{1}{L}(A_1 - A_0\alpha_j) r_j \,, \; a_{2j} = \frac{A_3}{L}(L - r_j\,\beta_j), \\
& a_{3j} = \frac{1}{L}(A_1\alpha_j - A_2) r_j \,, \; a_{4j} = -\frac{1}{L}(A_1 - A_0\alpha_j) r_j\, e^{r_j}, \\
& a_{5j} = -\frac{A_3}{L}(L - r_j\,\beta_j) e^{r_j}, \; a_{6j} = -\frac{1}{L}(A_1\alpha_j - A_2) r_j\, e^{r_j}
\end{aligned}
\right\} \tag{33}
$$

The 6×6 frequency dependent dynamic stiffness matrix can now be derived by eliminating the constant vector **R** from Equations (30) and (31) to give

$$
\mathbf{F} = \mathbf{K}\,\boldsymbol{\delta} \tag{34}
$$

where

$$
\mathbf{K} = \mathbf{A}\,\mathbf{B}^{-1} \tag{35}
$$

is the required dynamic stiffness matrix.

The dynamic stiffness matrix obtained in Equation (35) is used to compute natural frequencies and mode shapes of either an individual FGB or an assembly of FGBs with various boundary conditions.

2.3 Application of the Wittrick-Williams algorithm

A reliable and accurate method of computing the natural frequencies using the DSM is to apply the well-established Wittrick-Williams algorithm [13] which is ideally suited to solve transcendental eigenvalue problems such as the one in this paper. The algorithm uses the Sturm sequence property of the dynamic stiffness matrix and has featured in literally hundreds of papers. It ensures that no natural frequencies of the structure being analysed are missed. Clearly, this is not possible in the conventional finite element or other approximate methods. For a detailed insight of the algorithm, interested readers are referred to the original work of Wittrick and Williams [13].

3 Numerical results and discussions

Results are obtained for a wide range of the FGB with various boundary conditions. In order to make the results universal, the natural frequencies are non-dimensionalised as follows:

$$\lambda_i = \frac{\omega_i L^2}{h}\sqrt{\frac{\rho_b}{E_b}} \tag{36}$$

where ω_i is the ith angular natural frequency, ρ_b and E_b are the density and Young's modulus of the bottom surface material.

The theory developed here is now applied to an individual FGB for a number of classical boundary conditions. Based on the material property variation shown in Equation (1), numerical results were obtained for a range of FGB. The theory is sufficiently general and can be used for any constituent materials of the FGB. However, the example using aluminium (Al) and alumina (Al_2O_3) for the bottom and top surface materials respectively is illustrated here just for convenience. The material properties of the FGB are:
Al (bottom surface): E = 70 GPa, ρ = 2700 kg/m^3, ν = 0.23
Al_2O_3 (top surface): E = 380 GPa, ρ = 3800 kg/m^3, ν = 0.23

Although Poisson's ratio is kept constant, the theory developed can be used without this restriction. Numerical results for the natural frequencies and mode shapes are obtained for the FGB for three different boundary conditions, namely, simply-supported, clamped-clamped and cantilever. In order to check the validity and accuracy of the investigation, the results obtained from the analysis are compared with published ones. First, the special case of the FGB made of pure Al when $k = \infty$ is investigated. Table 1 shows the non-dimensional fundamental natural frequency of the FGB for three different length to thickness ratio L/h for simply-supported, clamped-clamped and cantilever boundary conditions. As expected, the fundamental natural frequency increases with the increase of the ratio L/h for all three boundary conditions. The results for the simply-supported boundary condition for which comparative results are available, agree very well with the ones reported in Ref [10], see results in parentheses.

L/h	Non-dimensional fundamental natural frequency (λ_1)		
	Simply-supported	Clamped-clamped	Cantilever
10	2.8024 (2.797)	6.0544	1.0070
30	2.8439 (2.843)	6.4096	1.0144
100	2.8496 (2.848)	6.4564	1.0153

Table 1: Non-dimensional fundamental natural frequency of a pure Al beam

The next set of results was obtained to show the effect of the length to thickness ratio L/h and the power-law distribution parameter k on the fundamental natural frequency of the FGB for various boundary conditions. Tables 2, 3 and 4 show the non-dimensional fundamental natural frequencies with respect to power-law distribution k and the ratio L/h for the simply-supported, clamped-clamped and cantilever boundary conditions, respectively. It can be seen that the fundamental natural frequency decreases with the increase of k for all three boundary conditions. This is to be expected because the material properties tend towards those of aluminium as k increases for which E/ρ is much smaller than alumina. Naturally, the highest fundamental natural frequencies are obtained for the case when $k = 0$ for which the FGB is made of full ceramic (Al_2O_3) whereas the lowest ones are obtained for the case $k = \infty$ when the FGB is made of full metal (Al). For a constant value of k, the fundamental natural frequencies increase when the ratio L/h increases as expected. It can be seen that there is no significant change on the fundamental natural frequency when the ratio L/h assumes higher values, for which Bernoulli-Euler theory will be adequate.

L/h	Non-dimensional fundamental natural frequency (λ_1)							
	Al_2O_3 ($k = 0$)	k						Al ($k = \infty$)
		k =0.2	k =0.5	k = 1	k = 5	k = 10	k = 20	
10	5.5071	5.1547	4.8383	4.5789	4.0647	3.7454	3.4211	2.8024
20	5.5707	5.2144	4.8940	4.6335	4.1244	3.8013	3.4699	2.8372
30	5.5905	5.2325	4.9109	4.6499	4.1412	3.8169	3.4838	2.8439
100	5.5996	5.2408	4.9187	4.6575	4.1496	3.8248	3.4907	2.8496

Table 2: Non-dimensional fundamental frequency of a simply-supported FGB

L/h	Non-dimensional fundamental natural frequency (λ_1)							
	Al_2O_3	k						Al
	($k = 0$)	k =0.2	k =0.5	k = 1	k = 5	k = 10	k = 20	($k = \infty$)
10	11.926	11.177	10.485	9.8894	8.6612	7.9850	7.3225	6.0544
20	12.476	11.680	10.952	10.346	9.1654	8.4605	7.7396	6.3095
30	12.604	11.796	11.061	10.452	9.2813	8.5698	7.8354	6.4096
100	12.687	11.872	11.131	10.520	9.3595	8.6437	7.8998	6.4564

Table 3: Non-dimensional fundamental frequency of a clamped-clamped FGB

L/h	Non-dimensional fundamental natural frequency (λ_1)							
	Al_2O_3	k						Al
	($k = 0$)	k =0.2	k =0.5	k = 1	k = 5	k = 10	k = 20	($k = \infty$)
10	1.9783	1.8513	1.7378	1.6455	1.4638	1.3486	1.2311	1.0070
20	1.9836	1.8615	1.7473	1.6548	1.4740	1.3583	1.2395	1.0112
30	1.9935	1.8659	1.7514	1.6587	1.4779	1.3618	1.2427	1.0144
100	1.9936	1.8673	1.7527	1.6600	1.4793	1.3632	1.2438	1.0153

Table 4: Non-dimensional fundamental natural frequency of a cantilever FGB

Table 5 shows the first three non-dimensional natural frequencies of a cantilever FGB for different power distribution parameter *k* when the ratio *L*/*h* is fixed at 10. It can be seen that the non-dimensional natural frequencies decreases with increasing *k*, as expected. The dimensionless natural frequencies of the FGB are larger when the beam is made of ceramic Al_2O_3. The natural frequencies are almost doubled.

No.	Non-dimensional fundamental natural frequency (λ_i)						
	Al_2O_3 ($k = 0$)	k =0.2	k =0.5	k = 1	k = 5	k = 10	Al ($k = \infty$)
1	1.9783	1.8513	1.7378	1.6455	1.4638	1.3486	1.0070
2	11.877	11.126	10.440	9.8597	8.6809	8.0017	6.0277
3	30.849	29.364	27.538	25.667	20.037	18.266	15.688

Table 5: Non-dimensional natural frequencies of a cantilever FGB for *L/h*=10

In order to establish trends, the effect of the *L*/*h* ratio on the fundamental natural frequency is shown graphically in Figure 3 for a set of *k* values when the FGB is simply-supported at the both ends. It can be seen that the fundamental natural frequency changes significantly when $L/h \leq 10$. When $L/h > 10$, the fundamental natural frequency is virtually unaltered.

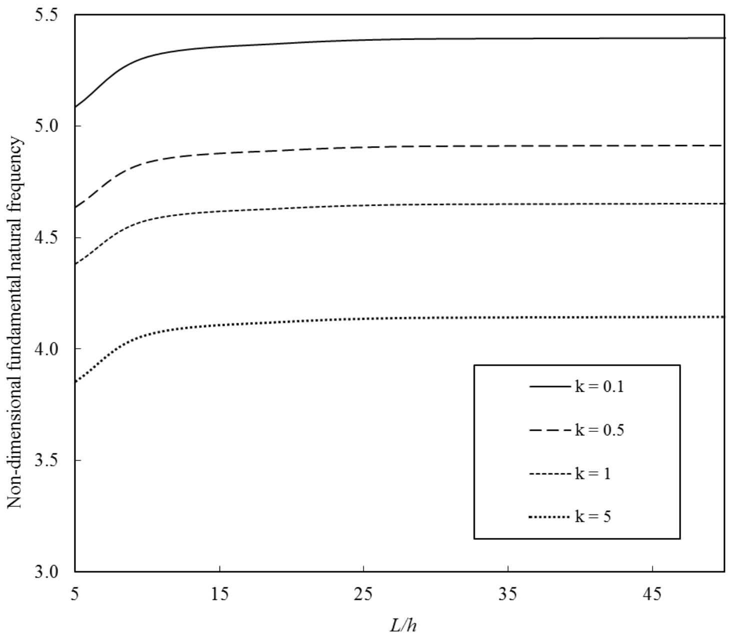

Figure 3: The effect of the ratio *L*/*h* on the fundamental natural frequency of a simply supported FGB.

To illustrate the effect of *k* on the fundamental natural frequency, Figure 4 shows the fundamental natural frequency of the simply-supported FGB for two different values of the *L*/*h* ratio. The power exponent *k* starts from zero when the construction of the FGB is made from pure alumina and tends towards aluminium when k assumes large values. The fundamental natural frequency is reduced as the value of *k* is increased. The same pattern for other *L*/*h* ratio was observed.

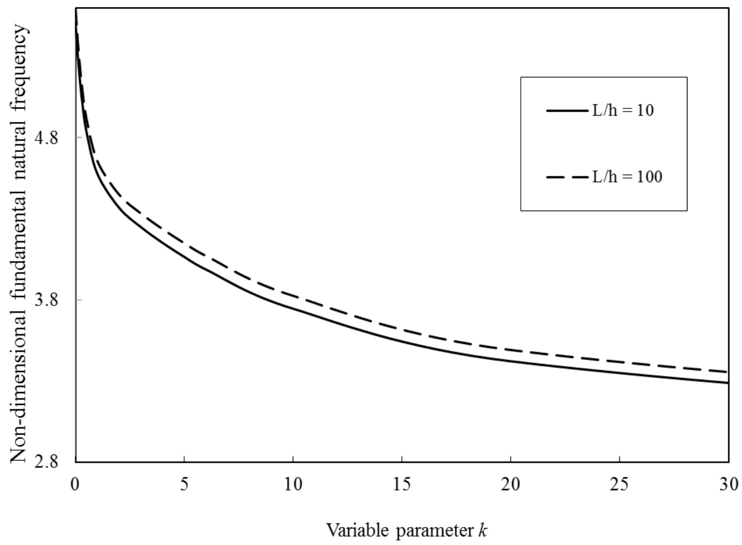

Figure 4: The effect of *k* on the fundamental natural frequency of a simply supported FGB

The final set of results was obtained to demonstrate the mode shapes of the FGB. Figure 5 shows the first three normalised mode shapes of the FGB for cantilever end conditions for two different *L*/*h* ratios when k = 0.5. The first two modes are dominated by bending displacements for both *L*/*h* = 10 and 20. The third mode is essentially an axial mode when *L*/*h*=10 whereas by contrast it becomes a bending mode when *L*/*h* =20. This is very interesting and can be useful in solving frequency attenuation problems.

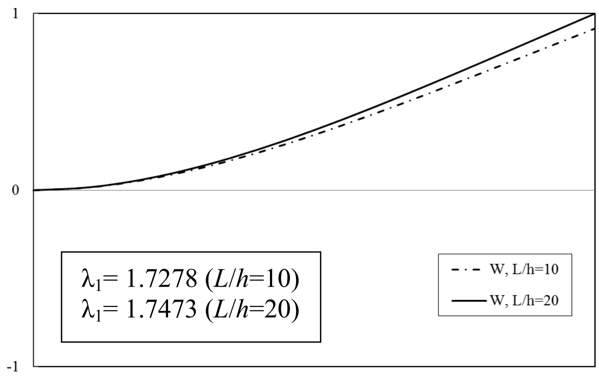

(a) The first mode shape

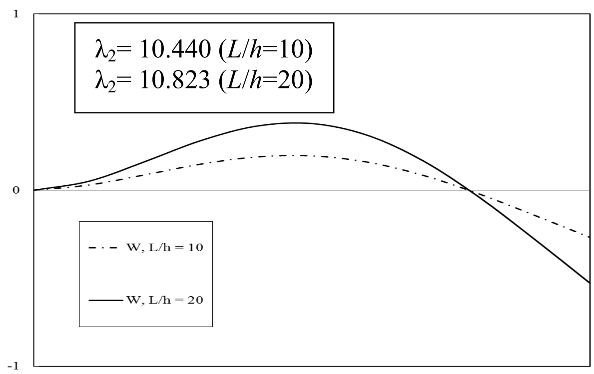

(b) The 2nd mode shape

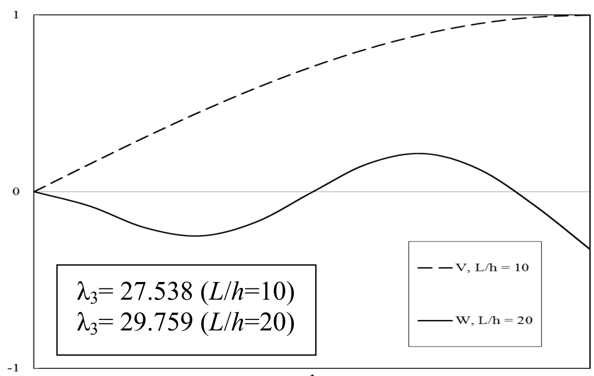

(c) The 3rd mode shape

Figure 5: Normalised mode shape for a cantilever FGB

4 Conclusion

Starting from the derivation of the governing differential equations of motion in free vibration, the dynamic stiffness matrix of a functionally graded beam using Timoshenko beam theory has been developed and applied with particular reference to the Wittrick-Williams algorithm to investigate its free vibration characteristics. Natural frequencies and mode shapes of some illustrative examples computed using the developed theory are discussed and compared with published ones. The investigation has revealed that by choosing the material distribution law and the length to thickness ratio in an appropriate way, it is possible to alter the natural frequencies and mode shapes in a significant way. This is particularly useful to solve frequency attenuation problems. The proposed method is computationally efficient and numerically accurate. The method gives exact results and can be used as an aid to validate finite element and other approximate methods.

References

[1] M. Simsek, "Fundamental frequency analysis of functionally graded beams by using different higher-order beam theories", Nuclear Engineering and Design, 240, 697-705, 2010.

[2] M. Aydogdu, V. Taskin, "Free vibration analysis of functionally graded beams with simply supported edges", Materials and Design, 28, 1651-1656, 2007.

[3] A. Chakrabort, S. Gopalakrishnan, J.N. Reddy, "A new beam finite element for the analysis of functionally graded materials", International Journal of Mechanical Science, 45, 519-539, 2003.

[4] C.F. Lu, W.Q. Chen, "Free vibration of orthotropic functionally graded beams with various end conditions", Structural Engineering and Mechanics, 13, 1430-1437, 2005.

[5] S. Kapuria, M. Bhattacharyya, A.N. Kumarb, "Bending and free vibration response of layered functionally graded beams: A theoretical model and its experimental validation", Composite Structures, 82(3), 390-402, 2008.

[6] Y. Huang and X.F. Li, "A new approach for free vibration analysis of axially functionally graded beams with non-uniform cross-section", Journal of Sound and Vibration, 329, 2291-2303, 2010.

[7] G. Giunta, D. Crisafulli, S. Belouettar, E. carrera, "Hierarchical theories for the free vibration analysis of functionally graded beams", Composite Structures, 94, 68-74, 2011.

[8] A.E. Alshorbagy, M.A. Eltaher, F.F. Mahmoud, "Free vibration characteristics of a functionally graded beam by finite element method", Applied Mathematical Modelling, 35, 412-425, 2011.

[9] H.J. Xiang, J. Yang, "Free and forced vibration of a laminated FGM Timoshenko beam of variable thickness under heat conduction", Composites: Part B, 39, 292–303, 2008.

[10] S.A. Sina, H.M. Navazi, H. Haddadpour, “An analytical method for free vibration analysis of functionally graded beams”, Materials and Design, 30, 741-747, 2009.
[11] Z. Zhong, T. Yu, “Analytical solution of a cantilever functionally graded beam”, Composites Science and Technology, 67, 481–488, 2007.
[12] J.R. Banerjee, A.J. Sobey, H. Su, J.P. Fitch, “Use of computer algebra in Hamiltonian calculations”, Advances in Engineering Software, 39, 521-525, 2008.
[13] W.H. Wittrick, F.W. Williams, “A general algorithm for computing natural frequencies of elastic structures”, Quart Journal of Mechanics and Applied Mathematics, 24, 263-284, 1971.